Fractalkine receptor deficiency impairs microglial and neuronal responsiveness to chronic stress

Giampaolo Milior [a,1], Cynthia Lecours [b,1], Louis Samson [b], Kanchan Bisht [b], Silvia Poggini [c], Francesca Pagani [d], Cristina Deflorio [a,e], Clotilde Lauro [a], Silvia Alboni [f], Cristina Limatola [a,g], Igor Branchi [c,2], Marie-Eve Tremblay [b,*,2], Laura Maggi [a,2]

[a] Department of Physiology and Pharmacology, Istituto Pasteur-Fondazione Cenci Bolognetti, Sapienza University of Rome, Italy
[b] Axe Neurosciences, Centre de recherche du CHU de Québec, 2705, boulevard Laurier, Québec, Canada
[c] Section of Behavioural Neurosciences, Department of Cell Biology and Neurosciences, Istituto Superiore di Sanità, Rome, Italy
[d] Center for Life Nanoscience, Istituto Italiano di Tecnologia@Sapienza, Rome, Italy
[e] Département de Neuroscience, Institut Pasteur, Unité Neurobiologie Intégrative des Systèmes Cholinergiques, Paris Cedex 15, Paris, France
[f] Department of Life Sciences, University of Modena and Reggio Emilia, Modena, Italy
[g] IRCCS Neuromed, Pozzilli, IS, Italy

A B S T R A C T

Chronic stress is one of the most relevant triggering factors for major depression. Microglial cells are highly sensitive to stress and, more generally, to environmental challenges. However, the role of these brain immune cells in mediating the effects of stress is still unclear. Fractalkine signaling – which comprises the chemokine CX_3CL1, mainly expressed by neurons, and its receptor CX_3CR1, almost exclusively present on microglia in the healthy brain – has been reported to critically regulate microglial activity. Here, we investigated whether interfering with microglial function by deleting the *Cx₃cr1* gene affects the brain's response to chronic stress. To this purpose, we housed *Cx₃cr1* knockout and wild-type adult mice in either control or stressful environments for 2 weeks, and investigated the consequences on microglial phenotype and interactions with synapses, synaptic transmission, behavioral response and corticosterone levels. Our results show that hampering neuron–microglia communication via the CX_3CR1–CX_3CL1 pathway prevents the effects of chronic unpredictable stress on microglial function, short- and long-term neuronal plasticity and depressive-like behavior. Overall, the present findings suggest that microglia-regulated mechanisms may underlie the differential susceptibility to stress and consequently the vulnerability to diseases triggered by the experience of stressful events, such as major depression.

1. Introduction

Major depression (MD) constitutes an enormous medical, individual, societal and economical challenge (Balak and Elmaci, 2007; Belmaker and Agam, 2008). One of the prominent causes of this burden is the very limited understanding of the processes underlying vulnerability to psychopathology. The quality of the living environment is among the largest risk factors for MD, with exposure to stressful events representing one of the most powerful triggers of depressive episodes (Cohen et al., 2007; Davidson and McEwen,

2012). However, this vulnerability differs between individuals. For instance, while serious life-threatening stress may not affect some individuals, milder stress triggers MD in others (Belsky et al., 2009; Caspi et al., 2003). The biological bases of such differential susceptibility to stress are still largely unknown.

Mainly recognized for their central role in the brain inflammatory response, microglia have recently emerged as cellular effectors linking the influence of the environment to the resulting modifications of brain function and behavior (Branchi et al., 2014; Walker et al., 2013). Equipped with receptors for a plethora of molecules, microglia are extremely sensitive to the ongoing experience (e.g. deprivation of visual stimuli, exposure to an enriched environment), to which they respond by modulating their surveillance of the brain parenchyma and their interactions with neuronal circuits (Paolicelli et al., 2014; Tremblay et al., 2010a).

In recent years, microglia–neuron interactions were also shown to regulate the maturation, function and modification of synapses, as well as adult neurogenesis (Paolicelli et al., 2011; Parkhurst et al., 2013; Schafer et al., 2012; Tremblay et al., 2010a). Though it is known that microglial phenotype is affected by chronic stress (Kierdorf and Prinz, 2013; Walker et al., 2013), the role of these immune cells in the neurobehavioral response to stress and in the pathogenesis of MD has remained elusive.

Among the candidate pathways which could underlie microglial response to the environment, fractalkine signaling is critical for mediating neuron–microglia crosstalk in various contexts of health and disease (Sheridan and Murphy, 2013). This chemokine is expressed by neurons, either as membrane-bound or soluble form, while its unique receptor CX_3CR1 is considered to be almost exclusively present on microglia in the healthy brain (Jung et al., 2000; Reaux-Le Goazigo et al., 2013), as infiltration of bone marrow-derived monocytes is marginal in normal physiological conditions (Gomez Perdiguero et al., 2015). Fractalkine signaling was recently found to control key microglial functions, such as the regulation of synaptic activity and the response to environmental stimuli, although some contradictory results are present (Bachstetter et al., 2011; Paolicelli et al., 2011, 2014; Reshef et al., 2014; Rogers et al., 2011; Wohleb et al., 2013; Zhan et al., 2014). Indeed, we have previously demonstrated that adult *Cx3cr1* knockout mice do not modify their neurobehavioral profile following a 10-week exposure to an enriched environment in contrast with what observed in wild-type mice (Maggi et al., 2011). In particular, *Cx3cr1* knockouts failed to enhance hippocampal CA1 long-term potentiation (LTP), the most commonly used paradigm of synaptic plasticity, and did not improve learning performance in the Morris water maze. More recently, these mice were also found to be resistant to anxiety-like behavior following repeated social stress, an effect attributed to a reduced brain infiltration of peripheral monocytes (Wohleb et al., 2013). These findings suggest that deletion of the *Cx3cr1* gene may prevent the modification of brain function and behavior induced by the environment.

The aim of the present study was to assess the role of microglia in transducing environmental stimuli into changes of brain function. In particular, we investigated the consequences of interfering with neuron–microglia communication, through fractalkine signaling deficiency, on brain responses to chronic unpredictable stress (CUS), an aversive condition reportedly leading to depressive-like behavior. Elucidating the neurobiological mechanisms underlying the differential susceptibility to stress may have paramount clinical implications for understanding the neural bases of psychopathologies triggered by environmental factors such as MD.

2. Materials and methods

2.1. Animals

All experiments were conducted in conformity with European Directive 2010/63/EU and the Italian D.lg. 4.05.2014, n. 26. Adult (12–16 weeks old) male mice were used: C57BL/6J wild-types and $CX_3CR1^{GFP/GFP}$ on a C57BL/6J background (from the Jackson Laboratory, Charles River, where the *Cx3cr1* gene was replaced by a green fluorescent protein (GFP) reporter) (Jung et al., 2000).

Twenty knockout and 20 wild-type mice were used. For each environmental condition (stress or control), 10 *Cx3cr1* knockout and 10 wild-type mice were housed together in the Intellicage system (TSE-system, NewBehavior AG, Zürich, Switzerland), which is an apparatus for the automated monitoring of mouse behavior (Fig. S1). This system is able to score the behavior of each individual living in a social group since each mouse is identified by a subcutaneous transponder. It consists of a large acrylic cage (20.5 × 58 × 40 cm, Model 2000 Tecniplast, Buguggiate, VA, Italy) with 4 conditioning chambers. Access to the chambers is provided via a tube with a built-in transponder codes reader (antenna). Each chamber contains two drinking bottles (see Fig. S1) accessible via openings with motorized doors. Poking a nose into the openings (nosepoke) activates an infrared beam break response detector. Three multicolor LEDs are mounted above each door and the nozzles of tubes are connected to tanks of compressed air located above each conditioning chamber deliver air puffs.

The Intellicage system collects data about the (i) number and duration of visits in the four corners (activity), (ii) number, duration and side (right or left) of nosepokes and (iii) number, duration and side (right or left) of licks. The floor is covered with bedding and contains four sleeping shelters in the center, on the top of which the animals may climb to reach food located in the feeder in the lid of the cage (food *ad libitum*). Each intellicage is connected through a tube to an escape box, a second Plexiglas box (30 × 20 × 15 cm) with metal tops and sawdust as bedding and food *ad libitum*.

2.2. Housing conditions

Mice were kept under a 12-h light–dark cycle at 22–25 °C. For the entire duration of each experiment, animals were housed in the Intellicage system. Five days before being moved to the Intellicage, each animal was injected with a subcutaneous transponder (T-IS 8010 FDX-B; Datamars SA, Switzerland). Food was freely available. The animals were gradually habituated to the Intellicage environment during a 14-day period (experimental scheme illustrated in Fig. 1). During such period, they were habituated also to a 0.1% of saccharin solution. On the last 2 days of the habituation period, the baseline for saccharin preference was measured.

2.2.1. Control and stressful conditions

In order to control for potential biases arising from alterations in social behavior reported in *Cx3cr1* knockout mice (Zhan et al., 2014), we housed mixed groups of experimental subjects (i.e., wild-type and *Cx3cr1*) in both the control and the stressful environment. This ensured that the differences measured were due to stressful experiences and not an artifact of the different social environments which may occur in *Cx3cr1* knockout mouse colonies. Control condition consisted in housing mice in the Intellicage for 2 weeks in the absence of stressful procedures. During this period, mice were habituated to a 0.1% of saccharin solution. In particular, during the first 4 days of Intellicage habituation, mice were exposed to the saccharin solution only (all bottles were filled with saccharin solution), while in the remaining 10 days mice chose between water and saccharin solution. Stressful condition consisted in exposing mice for 2 weeks to different stressful procedures administered by the Intellicage system in an automated fashion. The four stressful procedures each lasted 24 h: *Short open door*: doors to access both water and saccharin remain open for 1.5 s; *Open door 25%*: only 25% of nosepokes lead to door opening; *Air puff*: when the mouse enters the corner, it has a 20% chance of receiving an air puff; *Delay*: door to access water or saccharin solution opens only 2.5 s after the nosepoke. Each procedure was presented no more than 3 times. Exposing mice to different stressful procedures prevented habituation to stress. In addition, the escape box was removed during stressful conditions, adding on to the stress due to forced social interactions. Several CUS protocols using the Intellicage system have demonstrated its effectiveness in stressing experimental subjects, affecting anhedonia, corticosterone and BDNF levels (Branchi et al., 2013a,b).
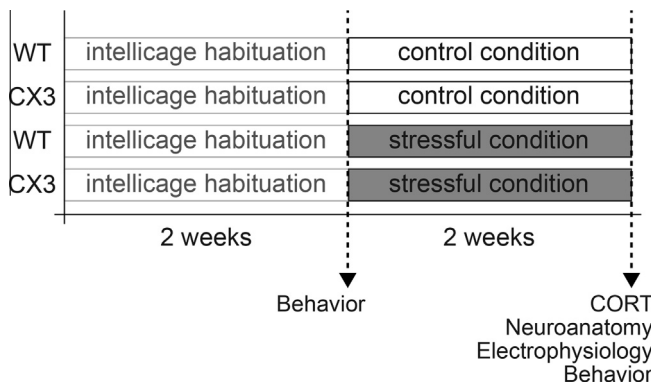
Fig. 1. Schematic representation of the experimental design and paradigm of chronic unpredictable stress used in our study.

2.3. Behavioral tests

To assess liking-type anhedonia we measured saccharin preference. In each corner of the Intellicage, two bottles were present, one containing tap water and the other containing 0.1% saccharin solution; both were freely available 24/24 h. Water and saccharin solution were substituted every day. The position of the water and saccharin bottles was counterbalanced across the four corners. Saccharin preference was determined as follows: (saccharin solution consumed/saccharin solution consumed + water consumed) × 100.

Activity score was measured as the number of corner visits.

2.4. Light and electron microscopy

2.4.1. Animals

For light and electron microscopy (EM) analyses, four mice per experimental group were anesthetized with sodium pentobarbital (80 mg/kg, i.p.) and perfused through the aortic arch with 0.1% glutaraldehyde in 4% paraformaldehyde (Ligorio et al., 2009). Only mice for which the perfusion was optimal were included in the study. Transverse sections of the brain (50 μm thick) were cut in sodium phosphate buffer (PBS; 50 mM at pH 7.4) using a vibratome and stored at −20 °C in cryoprotectant (30% glycerol and 30% ethylene glycol in PBS) until further processing (Tremblay et al., 2010b).

2.4.2. Immunoperoxidase staining

For light microscopy, sections were washed in PBS to remove the cryoprotectant, quenched with 2% H_2O_2 in 70% methanol for 10 min at room temperature (RT), washed in Tris–buffered saline (TBS; 50 mM at pH 7.4) containing 1% Triton X100, and processed freely-floating for immunoperoxidase staining. Briefly, sections were pre-incubated for 1 h at RT in a blocking solution of TBS containing 10% fetal bovine serum, 3% bovine serum albumin, and 1% Triton X100. They were incubated overnight at 4 °C in rabbit anti-IBA1 antibody (1:1000 in blocking solution; Wako Pure Chemical Industries) and rinsed in TBS. After incubation for 1.5 h at RT in goat anti-rabbit IgGs conjugated to biotin (1:200 in blocking solution; Jackson Immunoresearch) and for 1 h with A and B reagents of the ABC Vectastain system (1:100 in TBS; Vector Laboratories), the labeling was revealed using diaminobenzidine (DAB; 0.05%) and hydrogen peroxide (0.015%) in TBS for 5 min. Sections from all mice from all experimental groups (3–4 mice per group) were reacted together in multi-well dishes to ensure uniform experimental parameters, and all the analyses were conducted blind to the experimental conditions. For EM, sections were immunostained as mentioned above except that quenching was

first done with 0.3% H_2O_2 in PBS for 5 min and then with 0.1% $NaBH_4$ for 30 min, while the blocking buffer and antibody incubation solutions contained 0.01% Triton X100.

After immunostaining, sections for light microscopy were mounted onto glass slides, dehydrated in ascending concentrations of ethanol, cleared in citrisol, and coverslipped with DPX (Electron Microscopy Sciences; EMS). Sections for EM were post-fixed flat in 1% osmium tetroxide and dehydrated in ascending concentrations of ethanol. They were treated with propylene oxide, impregnated in Durcupan (EMS) overnight at RT, mounted between ACLAR embedding films (EMS), and cured at 55 °C for 72 h. Areas of CA1 stratum radiatum, at a level approximating the transverse planes Bregma −3.27 to −4.03 (Paxinos and Franklin, 2013), were excised from the embedding films and re-embedded at the tip of resin blocks. Ultrathin (65–80 nm) sections were cut with an ultramicrotome (Leica Ultracut S), collected on bare square-mesh grids, and examined at 80 kV with a FEI Tecnai Spirit G2 transmission electron microscope.

2.4.3. Light microscopy imaging and analysis

Color pictures were acquired in the CA1 stratum radiatum of 2 sections per mouse using an Infinity 2 camera (5 MP; Lumenera), at 10× for the cellular density and spacing analysis, and at 40× for the morphology analysis. All the analysis was performed with the ImageJ software (National Institutes of Health). To determine cellular densities and spacing, the CA1 stratum radiatum was delineated in 10× pictures by using the freehand selection tool, based on the stereotaxic atlas of Paxinos and Franklin (Paxinos and Franklin, 2013), and its area measured in pixels and converted into mm^2. The center of each microglial cell body (area ⩾ 20 μm^2) was marked with a dot using the paintbrush tool. The analyse particles function was used to automatically record cell numbers as well as spatial coordinates, enabling to determine the nearest neighbor distance for each cell with the nearest neighbor distance plugin. Total cell number was divided by the total area to determine cellular density on an animal basis. A spacing index was calculated as the square of the average nearest neighbor distance multiplied by microglial density per animal (Tremblay et al., 2012).

To analyse morphology, a total of 15 microglial cells per animal were analyzed at 40×. Only cells whose cell body and proximal processes were perfectly in focus were included in the analysis. Every IBA1-immunopositive microglia in a particular picture was analyzed before moving on to the next picture as to not introduce selection bias (Tremblay et al., 2012). For each microglia, the soma area was determined by drawing a line around the cell body by using the freehand selection tool. The arborization area was determined with the polygon selection tool to connect the most distal extremities of every process. The soma and arborization areas were calculated in pixels and converted into micrometers. A morphological index was determined by using the formula: soma area/arborization area (Tremblay et al., 2012).

2.4.4. Electron microscopy imaging and analysis

Pictures were randomly taken at 9300× in the CA1 stratum radiatum of each animal, for a total surface of ∼2000 μm^2 of neuropil captured per animal, using an ORCA-HR digital camera (10 MP; Hamamatsu). Cellular profiles were identified according to criteria previously defined (Peters et al., 1991; Tremblay et al., 2007, 2009, 2012). In addition to their IBA1 staining, microglial processes displayed irregular contours with obtuse angles, an electron-dense cytoplasm, numerous large vesicles, occasional multivesicular bodies, frequent phagocytic inclusions, distinctive long stretches of endoplasmic reticulum, and were typically surrounded by pockets of extracellular space (Tremblay et al.,

2010a). For quantitative analysis, each captured IBA1-positive microglial process was analyzed. A phagocytic index was compiled in Adobe Photoshop CS6 using pictures adjusted for brightness and contrast, by summing up the vacuoles and endosomes containing cellular materials such as membranes, axon terminals with 40-nm synaptic vesicles and dendritic spines with a postsynaptic density, on a microglial process basis (Tremblay et al., 2010a).

2.5. Corticosterone levels

Corticosterone levels were measured in all subjects after the 2 weeks of chronic stress procedure or in control condition at the same time point. Blood was collected from the tail 1 h before lights on. The bleeding procedure consisted in a small and superficial cut in the tail. Blood samples were collected individually in potassium–EDTA coated 10 ml tubes (1.6 mg EDTA/ml blood; Sarstedt, Germany). All samples were kept on ice and later centrifuged at 3000 rpm for 15 min at 4 °C. Blood plasma was transferred to Eppendorf tubes for corticosterone determination and stored at −80 °C until further analysis. Corticosterone was measured using a commercially available radio-immunoassay (RIA) kit containing 125 iodine labeled corticosterone (MP Biomedicals Inc., CA, USA). Vials were counted for 2 min in a gammascintillation counter (Packard Minaxi Gamma counter, Series 5000). Sensitivity of the assay was 0.125 mg/dl, inter- and intra-assay variation was less than 10% and 5%, respectively.

2.6. Electrophysiological analysis

2.6.1. Hippocampal slice preparation
Electrophysiological experiments were performed at the end of environmental stimulation (control or stressful condition) in acute hippocampal slices. Briefly, the animals were decapitated after being anesthetized with halothane. Whole brains were rapidly removed from the skull and immersed for 10 min in ice-cold artificial cerebrospinal fluid (ACSF) solution containing (in mM): NaCl 125, KCl 4.4, $CaCl_2$ 2.5, $MgSO_4$ 1.5, $NaHPO_4$ 1, $NaHCO_3$ 26 and glucose 10. The ACSF was continuously oxygenated with 95% O_2, 5% CO_2 to maintain the proper pH (7.4). Transverse 350 μm thick slices were cut at 4 °C with a vibratome (Thermo Scientific, USA) and the appropriate slices were placed in a chamber containing oxygenated ACSF. After their preparation, slices were allowed to recover for 1 h at 30 °C. For field recordings, individual slices were then transferred to the interface slice-recording chamber (BSC1, Scientific System Design Inc) with a total fluid dead space of approximately 3 ml. Slices were maintained at 30–32 °C and constantly superfused at the rate of 2.5 ml/min. Solutions were applied to the slices by a peristaltic pump. For the patch recordings, individual slices were transferred to the recording chamber and constantly superfused at RT at a rate of 1.5 ml/min.

2.6.2. Extracellular field recordings
At the beginning of each recording, a concentric bipolar stimulating electrode (SNE-100X 50 mm long Elektronik–Harvard Apparatus GmbH) was positioned in the stratum radiatum for stimulation of Schaffer collateral pathway projections to CA1. An ACSF-filled glass micropipette (0.5–1 MΩ) was positioned at 200–600 μm from the stimulating electrode for recording orthodromically-evoked field extracellular postsynaptic potential (fEPSP). Stimuli consisted of 100 μs constant square pulses, applied at 0.05 Hz. The intensity of the stimulus was adjusted in each experiment to evoke ∼50% of the maximal field potential amplitude without appreciable population spike contamination. Evoked responses were monitored online and stable baseline responses were recorded for at least 10 min. Only the slices that showed stable fEPSP amplitudes were included in the experiments. To analyze the time course of fEPSP slope, the recorded fEPSP was routinely averaged over 1 min ($n = 3$). LTP experiments were performed in ACSF and the protocol for the induction consisted in 3 HFS every 30 min (2 train 100 Hz, 1-s duration, 3-s inter-train interval) and the averaged fEPSP (25 min post-induction for each stimulation) was normalized to the baseline values (1 min).

For the paired-pulse ratio (PPR) test, closely spaced consecutive stimuli (50 ms interval) were used, and PPR was calculated as the ratio between the fEPSP amplitude evoked by the second stimulus (A2) over the first (A1; A2/A1). Input–output (I–O) curves of synaptic transmission were measured at the beginning of each experiment and were generated by applying a series of stimuli of increasing intensities to the Schaffer collaterals. fEPSP slopes were normalized to responses produced by the maximal stimulus intensity.

2.6.3. Data acquisition and analysis
Slices were visualized with a Wild M3B (Heerbrugg, Switzerland). fEPSPs were recorded and filtered (1 kHz) with an Axopatch 200 A amplifier (Axon Instruments, CA) and digitized at 10 kHz with an A/D converter (Digidata 1322A, Axon Instruments). Data were stored on a computer using pClamp 9 software (Axon Instruments) and analyzed off-line with Clamp-fit 9 program (Axon Instruments).

2.6.4. Patch clamp recordings
Whole-cell patch clamp recordings were performed at RT (23–25 °C) from CA1 pyramidal neurons in acute hippocampal slices after 1 h of recovery from the cut. Neurons were visualized at 40× with a Leica DM LFS microscope. Patch electrodes (3–4 MΩ) were made from borosilicate glass and filled with an intracellular solution containing (in mM): 140 Cs-methanesulphonate, 7 CsCl, 2 $MgCl_2$, 10 HEPES, 2 MgATP, 5 BAPTA; pH 7.3, with CsOH. Individual slices were constantly superfused with oxygenated (95% O_2, 5% CO_2; pH 7.4) ACSF containing (in mM): 125 NaCl, 2,5 KCl, 1,25 NaH_2PO_4, 1 $MgCl_2$, 2 $CaCl_2$, 26 $NaHCO_3$, 10 glucose. Recordings were made with a patch-clamp amplifier (Multicalmap 700 B; Molecular Devices, Foster city, CA), digitised through a Digidata 1440A A/D converter and acquired using pClamp 10.0 software (Axon Instruments, Union City, CA, USA). Neurons were clamped at −70 mV for sEPSC recordings. Recorded signals were low-pass filtered at 1 kHz and analyzed using Clampfit 10 software (Molecular Devices). Excitatory synaptic currents were identified on the basis of a template created for each neuron using 30–50 single events for each trace. All events recognized through the template search function were visualized, identified and accepted by manual analysis. Membrane capacitance was estimated as the total charge (i.e., the current integral, Qstep) mobilized in each cell by a 10 mV depolarizing step (Vstep): Qstep/Vstep.

2.7. Statistical analyses

All data were analyzed with 2-way ANOVAs, considering genotype and environmental condition (control, stress) as between-subject variables. For behavioral analysis, sample size was chosen to identify differences between experimental groups of about 0.9 times the standard deviation, in a two-way ANOVA with a two-sided alpha of 0.05 and a power of 0.80. In the case of distribution of phagocytic inclusions per microglial process the number of inclusions was considered as repeated measures within subjects. Post hoc comparisons were performed using the Tukey's HSD or the Holm–Sidak's tests. Where appropriate they were used in the absence of significant ANOVA results (Chiarotti et al., 1987;

Wilcox, 1987). Sample size (*n*) refers to individual animals for density and spacing index analyses and behavioral responses, while it refers to individual cells for morphological analysis and individual microglial processes for phagocytosis index analysis. For electrophysiological analyses, *n/N* refers to slices/mice. For subject randomization, three *strata* based on preference for saccharin after habituation and before exposure to the environmental conditions were created (medium, high-medium an high) in each group (wild-types and knockouts) and animals within each stratum were randomly assigned to each experimental group with restricted randomization in order to guarantee balance across treatment groups. Data were collected in a blind fashion. All values reported in the text are mean ± standard error of the mean (S.E.M.).

3. Results

We examined the effects of CUS and fractalkine signaling deficiency on microglial phenotype and synaptic/neuronal properties using light microscopy, electron microscopy, and electrophysiology. In addition, the effect of stress on corticosterone levels and anhedonia, a depressive-like behavior, was determined. Two groups of 10 adult wild-type and 10 adult *Cx₃cr1* knockout mice were housed in Intellicages, specially designed for automated monitoring and behavioral phenotyping with minimal human intervention. Following 2 weeks of habituation, mice were exposed either to a control or stressful environment for two additional weeks. We analyzed the CA1 hippocampal output region, stratum radiatum, which mediates mood and memory, and is profoundly affected by stress (Joels and Krugers, 2007).

3.1. Microglial phenotype

We evaluated microglial density and distribution in the CA1 radiatum by IBA1 immunostaining. We found that microglial density and spacing were not modified by CUS and fractalkine signaling deficiency, suggesting minimal proliferation or brain infiltration by IBA1-positive myeloid cells (Fig. 2a–b). By contrast, microglial cell body area [$F(1,221) = 25.169$, $p < 0.0001$] and arborization area [$F(1,221) = 8.549$, $p = 0.0038$] were increased in the *Cx₃cr1* knockout mice housed in both environments, indicating a difference in microglial basal properties between genotypes (Fig. 3a–b). Though the interaction genotype × environment failed to reach statistical significance for arborization area [$F(1,221) = 1.655$, $p = 0.1997$], *post-hoc* analysis revealed a reduction by stress only in the wild-types ($p < 0.05$). The genotype × environment interaction for morphological index was statistically significant [$F(1,221) = 11.465$, $p < 0.0008$] and *post-hoc* analysis revealed that, in control conditions, the *Cx₃cr1* knockouts show an increased morphological index compared to wild-types ($p < 0.01$), reflecting a bigger cell body with respect to the arborization area. This parameter was modified by stress only in the wild-type animals ($p < 0.05$).

The hippocampus CA1 radiatum was examined with electron microscopy and a phagocytic index was compiled by counting the number of phagocytic inclusions (i.e. cellular material being digested, including pre-synaptic axon terminals and post-synaptic dendritic spines) per IBA1-positive microglial process (see Fig. 4a–d for examples). The quantitative analysis revealed that wild-type mice display an increased number of microglial inclusions following housing in the stressful versus control environment (Fig. 4e). The number of microglial inclusions was also elevated in the *Cx₃cr1* knockout mice under control conditions, but it remained unchanged by chronic stress (Fig. 4e), contrary to the data gathered in wild-type mice. This indicates that the experience-dependent remodeling of neuronal circuits is impaired

at the synapse in the *Cx₃cr1* knockout animals. Additionally, the distribution of phagocytic inclusions per microglial process showed an increased prevalence of processes without inclusions in the wild-type controls, and of processes with 1–5 inclusions in the *Cx₃cr1* knockouts, under control and stressful conditions. These observations suggest that the increased basal microglial phagocytosis in the knockouts could interfere with their modulation by stress.

3.2. Synaptic/neuronal properties

To investigate the possible repercussion of these changes in microglial function on the synaptic and neuronal properties (see Kettenmann et al., 2013; Paolicelli et al., 2014; Tremblay et al., 2011), we performed electrophysiological recordings on acute hippocampal slices. We first investigated Schaffer collateral-CA1 synaptic strength by recording field extracellular postsynaptic potential (fEPSP) input–output (I–O) curves of synaptic transmission (Fig. 5a). Our results revealed that CUS does not affect I–O regardless of genotype and environmental conditions, indicating similar synaptic strength between the four groups. It has been reported that stress exposure increases glutamate release in the CA1 region (Venero and Borrell, 1999). We thus measured the Paired Pulse Ratio (PPR), a form of short-term plasticity related to neurotransmitter release probability (Zucker, 1989) by stimulating the Schaffer collateral projections to CA1 at 50 ms intervals, and determined the ratio between the amplitude evoked by a second stimulus over the first. As shown in Fig. 5b, CUS significantly reduces PPR only in wild-type mice ($p = 0.040$) suggesting an increased glutamate release probability. This result was also confirmed in patch clamp recordings (Fig. 6c).

Chronic stress has been reported to impair synaptic plasticity in the CA1 region (Alfarez et al., 2003). We explored LTP stimulating Schaffer collaterals with spaced (3 times, 30 min apart) high frequency stimulation (HFS) and analyzing LTP amplitudes 25 min after each stimulation. As presented in Fig. 5c and d, in the control condition, *Cx₃cr1* knockout animals show a trend to display higher levels of LTP compared to wild-type animals (*post-hoc*, $p = 0.073$), supporting previous findings (Maggi et al., 2011). Following the first stimulation, the stress protocol significantly reduces LTP amplitude in both genotypes (about 18%; *post-hoc*, $p < 0.05$; Fig. 5c and d). Interestingly, the main effects of genotype and the environment emerged during the second [respectively, $Fs(1,32) = 6.53, 4.37$, $ps = 0.016, 0.045$] and third stimulations [respectively, $Fs(1,21) = 4.73, 4.69$, $ps = 0.040, 0.0420$] though the interaction genotype × environment failed to reach statistical significance. *Post-hoc* analysis revealed that, at the second and third stimulations, CUS significantly reduces LTP expression only in wild-type mice ($p = 0.050$ and $p = 0.049$, respectively; Fig. 5c and d). It is noteworthy that following CUS the increase in synaptic weight due to repeated spaced HFS was lower in the wild-type animals compared to *Cx₃cr1* knockout animals reaching LTP saturation level after the second stimulation (136% of baseline).

To investigate possible functional alterations in the basal properties of pyramidal neurons we performed patch clamp recordings in the CA1 region. In line with previous findings (Karst and Joels, 2007), following CUS in the wild-type mice we observed a significant increase of cell capacitance ($p = 0.040$, Fig. 6a), suggesting an increase in the size of the soma and primary dendrites (Anderson et al., 2001), accompanied by a reduction of input resistance (R_{input}) in response to negative current injections ($p = 0.043$, Fig. 6b). In contrast, the *Cx₃cr1* knockout mice did not shown modulation of cell capacitance and R_{input} upon CUS exposure (Fig. 6a and b). We further measured spontaneous glutamatergic activity (EPSC) from patch-clamped neurons to assess possible
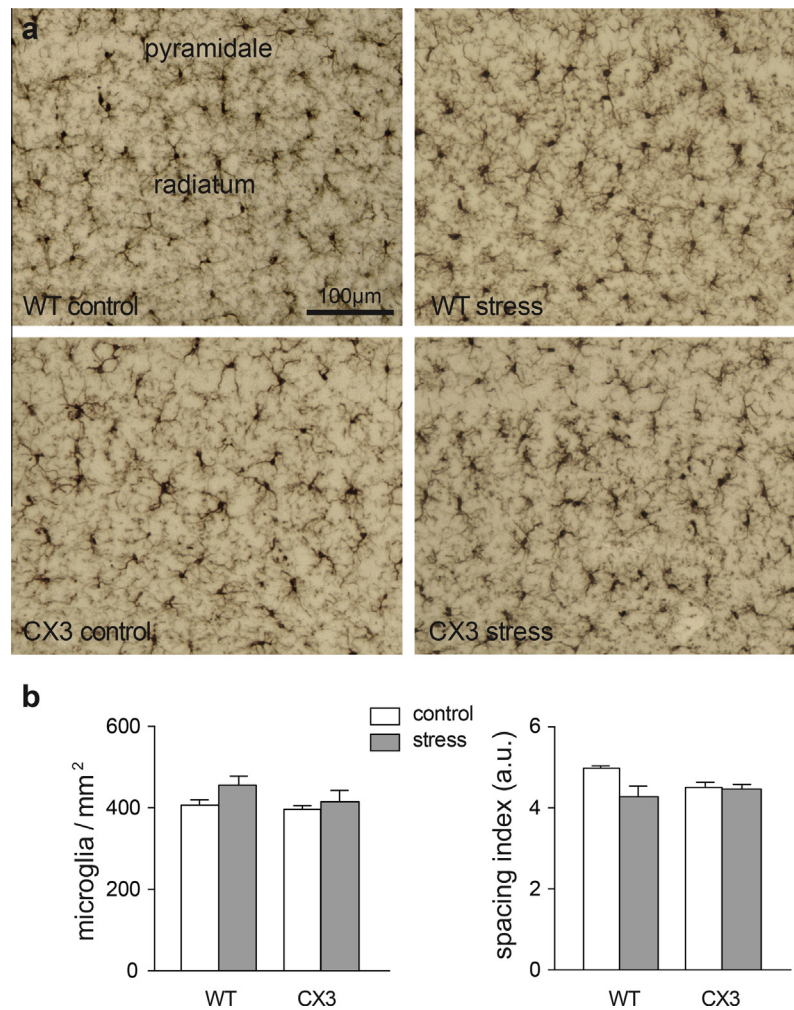
Fig. 2. Effects of chronic unpredictable stress on microglial density and spacing in CA1 radiatum. (a) Low magnification (10×) pictures showing IBA1-stained microglia in the four groups: wild-types (WT) and Cx_3cr1 knockouts (CX3) housed in control or stressful environments. (b) Microglial density and spacing in the four groups (n = 3–4 mice per group). a.u. = arbitrary units.

changes in neurotransmission. The average amplitude and frequency of EPSCs were not different between genotypes (Zhan et al., 2014) and were not affected by CUS exposure (Fig. S2), corroborating previous findings that AMPAR-mediated excitation is not decreased at the Schaffer Collateral-CA1 synapse following chronic stress (Kallarackal et al., 2013).

3.3. Anhedonia and corticosterone levels

As expected we found that exposure to CUS induces liking-type anhedonia in wild-type animals which showed a decrease in the preference for saccharine sweetened drinking water. Conversely, knockout animals did not display liking-type anhedonia (Fig. 6d). Though the interaction genotype × environmental condition did not reach statistical significance [$F(1,25)$ = 3.045, p = 0.093], post hoc analysis revealed that only wild-type mice show a decrease in their preference for saccharine-solution when exposed to chronic stress ($p < 0.05$). The two groups did not differ in locomotion levels, confirming that the lack of stress-induced anhedonia in the knockout mice is not activity based (Fig. 6e) (Schweizer et al., 2009). In addition, blood corticosterone levels were measured at the end of the exposure to the environmental conditions. As expected, mice exposed to CUS showed significantly higher levels of corticosterone than mice exposed to control conditions

[$F(1,23)$ = 6.727, p = 0.002]. However, no difference was found between Cx_3cr1 knockout and wild-type animals (Fig. 6f).

4. Discussion

The present findings show that fractalkine signaling deficiency prevents microglial and neuronal response to CUS. In particular, contrary to wild-type mice, Cx_3cr1 knockout mice failed to modify microglial morphology, phagocytosis of cellular elements, short- and long-term neuronal plasticity, or basal properties of pyramidal glutamatergic neurons in the hippocampus CA1 upon stress. In addition, knockouts showed no increase of liking-type anhedonia in response to stress. However, circulating corticosterone levels were similarly increased in both genotypes, indicating that the Cx_3cr1 knockout mice have a functionally intact hypothalamic–pituitary–adrenal axis. This suggests that the lack of changes in brain function may not be ascribed to a different sensitivity to stressful conditions but to a dysregulation of microglia–neuron crosstalk controlling the response to stress. The difference in neural and behavioral response, notwithstanding a similar increase in circulating corticosterone levels in the two experimental groups, could be attributed to a reduction in the hormone central levels or to an alteration of the interaction between glucocorticoid receptor and Cx_3cl1 function (Bhavsar et al., 2008). Further studies aimed at
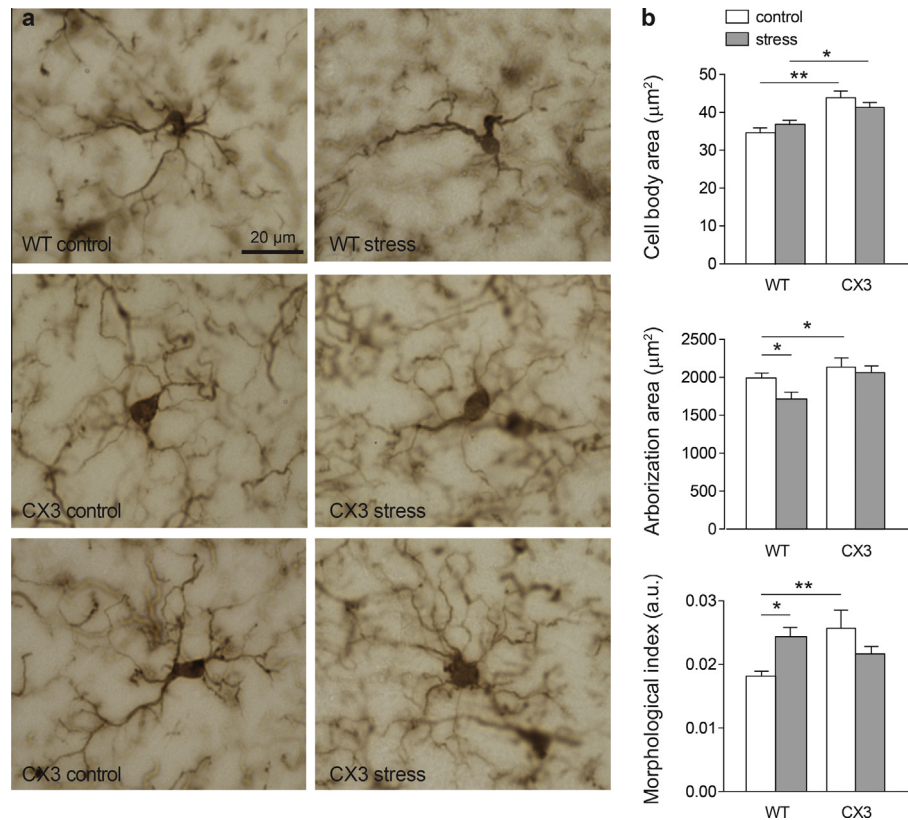
Fig. 3. Effects of chronic unpredictable stress on microglial cell body and arborization area, and morphological index in CA1 radiatum. (a) High magnification (40×) pictures showing the morphology of IBA1-stained microglia in the four groups, with two additional examples for the CX3. (b) Microglia cell body area, arborization area, and morphological index in the four groups (n = 45–60 microglial cells in 3–4 mice per group). a.u. = arbitrary units. $^*p < 0.05$ and $^{**}p < 0.01$.

investigating brain corticosterone levels and the possible modification of the glucocorticoid, as well as the mineralocorticoid receptor function in Cx_3cr1 knockouts are warranted.

4.1. Effects of chronic unpredictable stress on microglia and neurons

Previous studies reported that chronic stress affects microglia and neurons, driving the emergence of various changes that, according to the brain region examined and the nature and time-course of the stressor (Hinwood et al., 2012, 2013; Kreisel et al., 2014; Tynan et al., 2010; Wohleb et al., 2013), comprise microglial "activation", dendritic retraction accompanied by dendritic spine loss, as well as long-term plasticity reduction and glutamate release increase (Alfarez et al., 2003; Kreisel et al., 2014; Mayhew et al., 2015; Musazzi et al., 2011; Nasca et al., 2014; Sandi, 2011; Venero and Borrell, 1999; Walker et al., 2013) (Hinwood et al., 2012, 2013; Kreisel et al., 2014; Tynan et al., 2010; Wohleb et al., 2013). Here we show that in wild-type mice exposure to CUS reduces microglial arborization area and increases their morphological index (soma area/arborization area). Since microglial soma area did not vary significantly, the changes in morphological index most likely resulted from a reduction in arborization area. Similar alterations have been described during normal aging (Tremblay et al., 2012). We also show for the first time that microglial phagocytosis of cellular elements, including axon terminals and dendritic spines, is increased by CUS in wild-type mice. Previously, this process has been characterized in the visual cortex, where it was found to be exacerbated by 1 week of housing in complete darkness (Tremblay et al., 2010a), a potentially stressful environmental challenge (Keck et al., 2008; Majewska and Sur, 2003). This increased microglial phagocytosis of cellular elements is in line with the shortening of apical dendritic branches and loss of dendritic spines described in several brain regions, including the hippocampus CA1, following chronic restraint stress, exposure to predator odor, social defeat, corticosterone administration and in MD postmortem human brains (Alfarez et al., 2008; Cook and Wellman, 2004; Donohue et al., 2006; Duman and Aghajanian, 2012; Liston et al., 2013; Magarinos and McEwen, 1995; Pawlak et al., 2005; Penzes et al., 2011; Radley et al., 2004,, 2006). These observations suggest that microglial phagocytosis of synaptic elements is critically involved in the remodeling of neuronal circuits which underlies the brain's response to chronic stress (Luine et al., 1994; McEwen, 2007; Yoon et al., 2008; Yuen et al., 2012). In future studies, it will be important to identify the neurotransmitter contents of the pre-synaptic elements that are phagocytosed by microglia, to clarify their consequences on the activity of neuronal circuits. Indeed, alterations in the excitation/inhibition ratio represent a common pathway underlying several disorders including depression and autism (Rubenstein and Merzenich, 2003; Shabel et al., 2014).

Our findings also show that CUS affects neuronal properties, likely through its modification of cell capacitance, input resistance, PPR and LTP. Indeed, cell capacitance was enhanced in wild-type mice exposed to CUS compared to control conditions, suggesting that aversive stimulation could increase the surface of the soma or primary dendrites. Accordingly, chronic stress has been recently reported to induce atrophy selectively in the apical dendrites of CA1 pyramidal neurons (Christian et al., 2011). The variation in cell capacitance was accompanied by a reduction in input resistance, which is dependent on cell conductance and is inversely correlated with cell size. Overall, these results are in line with previous studies reporting that stress produces a 20–25% reduction in input
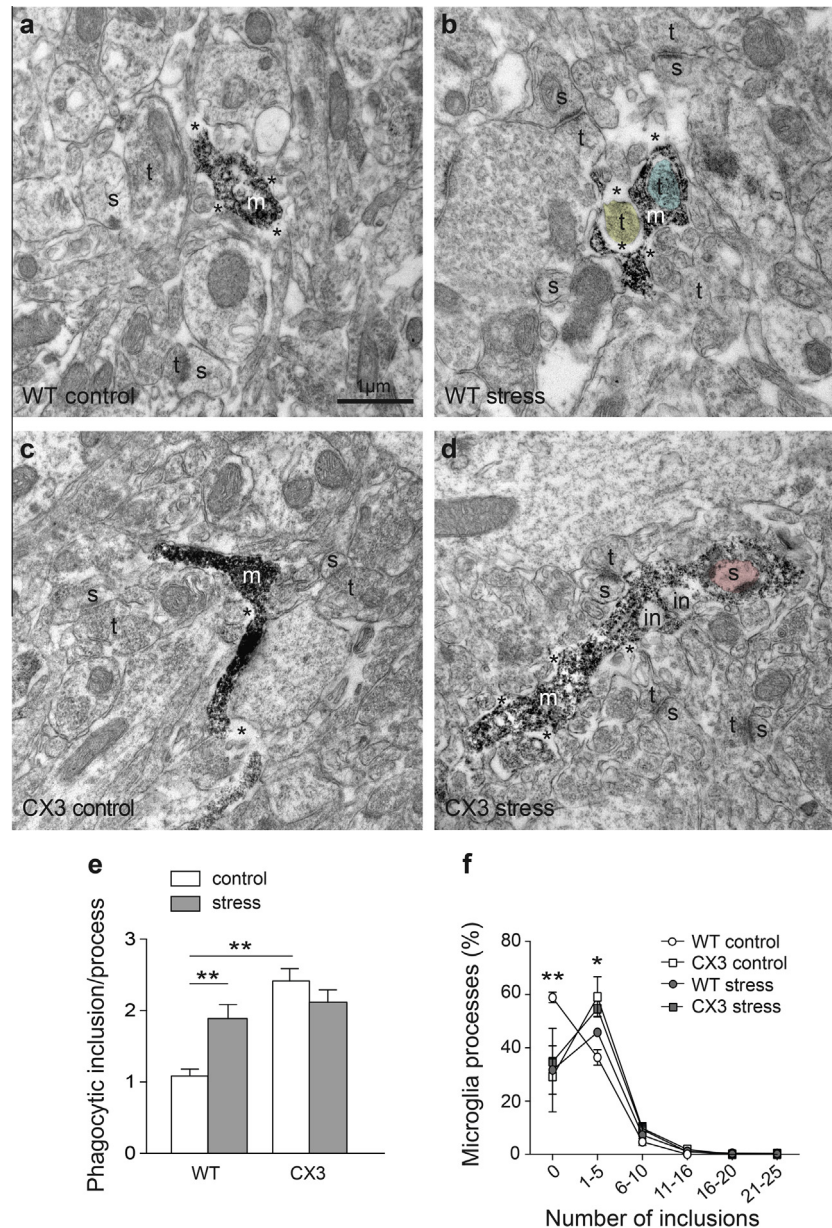
Fig. 4. Effects of chronic unpredictable stress on microglia phagocytosis of synaptic elements in CA1 radiatum. (a–d) Electron microscopy pictures showing examples of IBA1-stained microglial processes with bulky (a and d) and spindly (b and c) morphologies, as well as containing phagocytic inclusions with ultrastructural features of pre-synaptic axon terminals (b) or post-synaptic dendritic spines (d), as observed in the CX3 and WT mice in both environments. In (b), an axon terminal (t, colored in blue) is completely internalized by a microglial process, while another one (colored in yellow) is being engulfed. In (d), the microglial process contains a dendritic spine (s, colored in pink) recognized by its post-synaptic density as well as two additional inclusions (in) in a more advanced state of digestion. Extracellular space surrounding the microglia is shown by asterisks. (e) Quantitative analysis of the phagocytic index, measured as the number of inclusions (i.e. digested cellular materials, synaptic elements) per microglial process, in the four groups ($n = 244$–361 processes in 3 mice per group). (f) Distribution of the number of phagocytic inclusions per microglial process in the four groups ($n = 3$ mice per group). $^{*}p < 0.05$, $^{**}p < 0.01$.

resistance of CA3 pyramidal neurons (Kole et al., 2004) and a 30% increase in cell capacitance of CA1 neurons (Karst and Joels, 2007). The functional significance of these changes is still unclear and warrants further investigation. Exploiting extracellular and single-cell recordings, we demonstrated that PPR, a form of short-term plasticity related to probability release, is reduced by CUS in the CA1 of wild-type mice, indicating an increased probability of glutamate release at the Schaffer collateral synapse and corroborating previous findings that chronic stress increases glutamate levels in this region (Musazzi et al., 2011; Venero and Borrell, 1999). In line with the literature (Joels and Krugers, 2007; Kim and Diamond, 2002), we found that the classical type

of long-term plasticity, CA1 LTP, is affected by CUS. In addition, we extended previous findings and analyzed the effects of CUS on repetitive spaced HFS. Successive episodes of LTP have a cumulative effect on synaptic strength (Petersen et al., 1998), gradually increasing the degree of LTP induction until saturation. Our results show that CUS induces a form of metaplasticity, significantly reducing the amount of potentiation measured after spaced HFS and leading to LTP saturation already after the second HFS. Such incapacity to produce cumulative LTP in stressed mice could be due to the prevalence of synapses operating close to saturation. In addition, since it has been proposed that a gradual increase in population LTP may reflect the recruitment of additional synapses
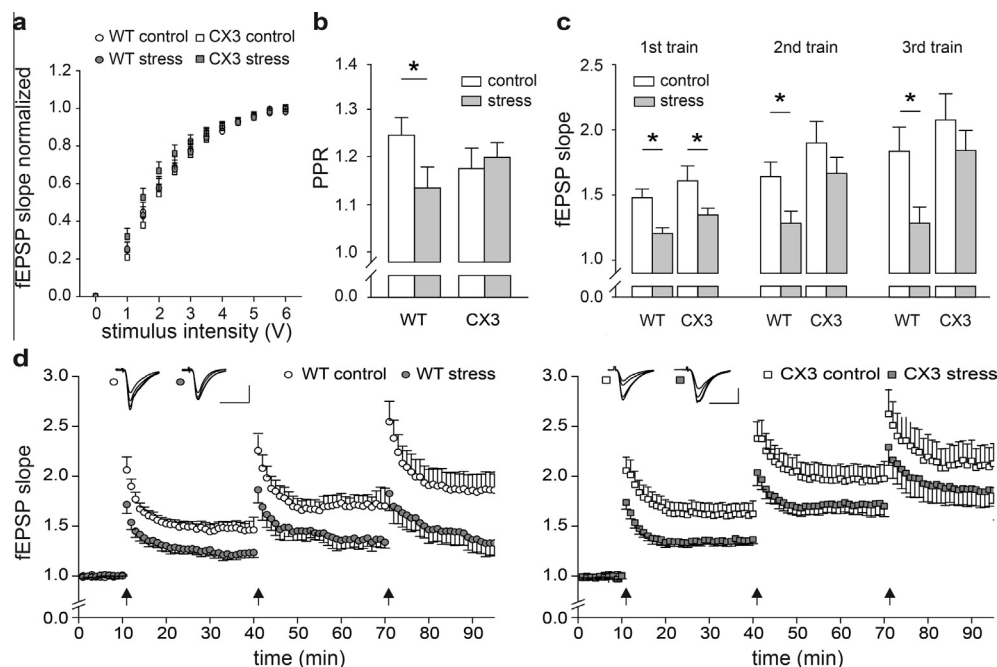
Fig. 5. CA1 basal responses and synaptic plasticity in WT and CX3 mice upon chronic unpredictable stress (a) Normalized stimulus intensity response curves (I–O) of WT and CX3 mice exposed to either control or stressful conditions (n = 9–12 slices/4–6 mice per group). (b) Paired Pulse Ratio (PPR) measurements (n = 17–21 slices/5–6 mice per group) (c and d) LTP saturation in WT and CX3 mice exposed either to control or stressful condition (n = 6–14 slices/5–6 mice per group) (c) Bar histogram of data points in (d) as averaged 25, 55 and 85 min after the HFS and normalized with respect to baseline (d) normalized averaged amplitudes of fEPSPs. Arrows indicate repeated spaced HFS. Field potential waveforms (averages of three traces) were taken at the times indicated by numbers. $^{*}p$ < 0.05.
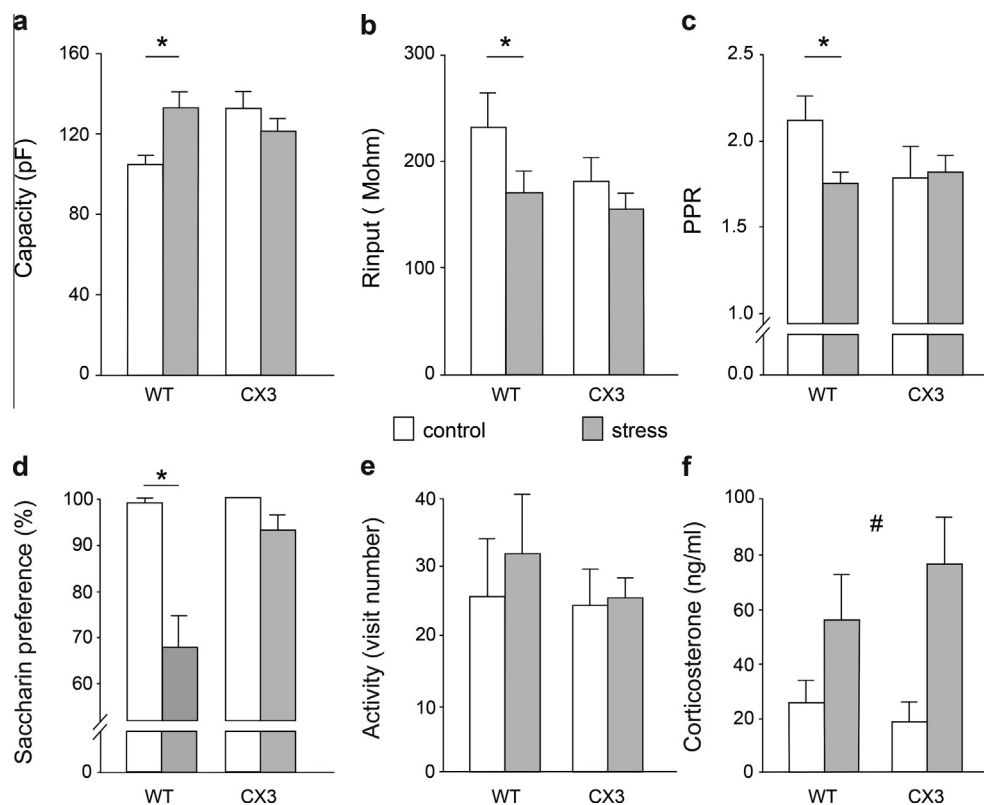

Fig. 6. Single cell and behavioral responses in WT and CX3 mice exposed to chronic unpredictable stress. (a–c) Cell capacitance, R input and PPR of WT and CX3 mice exposed to either control or stressful conditions (for cell capacitance and R input: n = 31–41 slices/5–6 mice per group; for PPR: n = 8–22 slices/3–5 mice per group). (d–e) Anhedonic behavior measured with the saccharin preference test, as well as locomotor activity in the four groups (n = 6–9 mice per group). * indicates p < 0.05. (f) Corticosterone levels in the four groups (n = 4–9 mice per group). # indicates the main effect of environment (p = 0.016).

with each train of impulses (Petersen et al., 1998), the unavailability of non-potentiated synapses in mice exposed to stress could explain the lack of a cumulative effect of repeated LTP. This is concordant with our data demonstrating an increased microglial phagocytosis of synaptic elements in stressed mice as well as previous studies showing a decreased number of dendritic spines as a consequence of chronic stress exposure (Alfarez et al., 2003; Donohue et al., 2006).

4.2. Fractalkine signaling deficiency alters microglial and neuronal properties

Under control conditions, the microglia of *Cx₃cr1* knockout mice differed from those of wild-type mice in many measures, showing increased cell body and arborization area, morphological index, and phagocytic inclusion of axon terminals and dendritic spines. Similarly, microglia within the dentate gyrus of *Cx₃cr1* knockout animals were recently shown to have increased cell body area compared to nontransgenic mice (Reshef et al., 2014). To the best of our knowledge, microglial arborization area and phagocytic activity have not been previously characterized in mature *Cx₃cr1* knockout mice during normal physiological conditions. These results show that *Cx₃cr1* knockout mice display immature- or reactive-like morphologies similar to those described during normal postnatal development of the hippocampus (Dalmau et al., 1998) a time of intense neuronal circuit remodeling and exacerbated microglial phagocytosis of synaptic elements (Bilimoria and Stevens, 2015; Paolicelli et al., 2014). This finding is in line with the idea that fractalkine communication is an "off" signal keeping microglia in a "resting" state (Biber et al., 2007). The role of microglia in synaptic pruning has previously been demonstrated in the *Cx₃cr1* knockouts, showing that a reduced number of microglia in the CA1 radiatum accompanies a transient increase in dendritic spine density, indicating that microglia are necessary for pruning during early postnatal development (Paolicelli et al., 2011). However, the consequences of fractalkine signaling deficiency on microglial phagocytosis of synaptic elements at adulthood remained undetermined.

In agreement with previous studies (Maggi et al., 2011) but at discrepancy with Rogers et al. (2011), *Cx₃cr1* knockout animals also showed a trend towards increased neuronal LTP. The reason for these contradictory results in LTP is not clear but could be related to differences in the ages, diet and housing conditions of the animals, or electrophysiological preparation between studies. In line with our results, Reshef et al. (2014) have also recently demonstrated that *Cx₃cr1*-deficient mice display better hippocampal-dependent memory.

4.3. Role of fractalkine signaling in the response to chronic unpredictable stress

The main finding of the present paper is that deficiency in fractalkine signaling leads to a lack of responsiveness of the brain and behavior to chronic stress. We have previously demonstrated that *Cx₃cr1* knockout mice do not respond to environmental enrichment (Maggi et al., 2011). In particular, *Cx₃cr1* knockout mice fail to demonstrate enhanced CA1 LTP following enrichment contrary to wild-type mice. Here, we show that *Cx₃cr1* knockout mice are similarly unaffected by an aversive environmental challenge. Supporting our findings (Maggi et al., 2011), Reshef et al. (2014) have recently shown that environmental enrichment does not produce improvement of memory functioning in the *Cx₃cr1* knockout mice. In the present study, exposure to chronic stress did not modify microglial or neuronal properties, and did not induce anhedonic response. In particular, *Cx₃cr1* deletion prevented the effects of CUS on microglial arborization area, morphological index, and

phagocytic elimination of neuronal/synaptic elements, as well as on neuronal properties such as cell capacitance, input resistance and PPR. Furthermore, *Cx₃cr1* deletion partially averted the effects of CUS on hippocampal LTP potentiation, hampering saturation following repeated spaced HFS. Finally, knockout mice did not display liking-type anhedonia, an index of depression-like behavior, in response to stress. A more comprehensive behavioral analysis is warranted for detailed phenotyping of the depression-like response.

Overall, in agreement with the previous findings (Branchi et al., 2014; Kreisel et al., 2014; Muller, 2014; Sierra et al., 2014b), these results indicate that microglia are key players at the interplay between environmental stimulation and brain function, being crucial for regulating the response to chronic stress. In addition, our results suggest that the altered crosstalk between neurons and microglia induced by fractalkine pathway silencing results in abnormal neuronal and microglial function, and disrupts the finely-tuned response of the brain to the ever-changing external environment.

Further studies are warranted to characterize the mechanisms underlying the effects of microglial *Cx₃cr1* deletion. Among the key molecular mediators which could be recruited downstream of CX₃CR1, interleukin-1β is of particular interest considering that its levels are regulated by fractalkine signaling (Bachstetter et al., 2011; Clark et al., 2015; Rogers et al., 2011) and chronic stress (Wohleb et al., 2013). This microglia-secreted cytokine may thus contribute to the effects of chronic stress on brain function and behavioral responses (Sierra et al., 2014a), including anhedonia (Goshen et al., 2009; Koo and Duman, 2008). Other mechanisms underlying stress resilience/resistance in the CX₃CR1 knockout mice should be considered, including modulation by other cytokines, trophic factors, inflammasome targets, and matrix metalloproteinases (MMPs) that have been recently associated with strain resistance to stress (Franklin et al., 2012; Hodes et al., 2012; Pfau and Russo, 2015). In addition it would be interesting to explore whether the reported differences are also present in other brain regions affected by stress, and the possible contribution of bone marrow-derived myeloid cells – besides to the endogenous microglia – to the observed effects.

In conclusion, elucidating the role of microglia in controlling brain responses to the environment may help to understand the neural bases underlying the differential inter-individual susceptibility to adverse challenges shown by the human population (Belsky and Pluess, 2009). In particular, it may be speculated that interfering with microglial function may render individuals less susceptible to the detrimental consequences of chronic stress and may reduce their vulnerability to mental disorders that are triggered by harsh environmental conditions, including MD. This study suggests a mechanistic basis for the development of innovative pharmaceutical agents to treat psychopathologies. In particular, the *Cx₃cl1*–*Cx₃cr1* signaling pathway, and consequently microglial activity, may be pharmacologically modulated in order to dampen the effects of the environment on the brain according to the potential consequences of its influence on mental health (Branchi, 2011). Such modulatory effects of microglia on the susceptibility to stress may represent the mechanisms of action of drugs known to affect both microglial activity and depression such as the antibiotic minocycline (O'Leary et al., 2015).

Conflict of interest

All the authors declare that there are no competing financial interests in relation to the work described.

Acknowledgments

Appendix A. Supplementary data

Supplementary data associated with this article can be found, in the online version, at http://dx.doi.org/10.1016/j.bbi.2015.07.024.

References

Alfarez, D.N., Joels, M., Krugers, H.J., 2003. Chronic unpredictable stress impairs long-term potentiation in rat hippocampal CA1 area and dentate gyrus in vitro. Eur. J. Neurosci. 17, 1928–1934.

Alfarez, D.N., Karst, H., Velzing, E.H., Joels, M., Krugers, H.J., 2008. Opposite effects of glucocorticoid receptor activation on hippocampal CA1 dendritic complexity in chronically stressed and handled animals. Hippocampus 18, 20–28.

Anderson, R.L., Jobling, P., Gibbins, I.L., 2001. Development of electrophysiological and morphological diversity in autonomic neurons. J. Neurophysiol. 86, 1237–1251.

Bachstetter, A.D., Morganti, J.M., Jernberg, J., Schlunk, A., Mitchell, S.H., Brewster, K.W., Hudson, C.E., Cole, M.J., Harrison, J.K., Bickford, P.C., Gemma, C., 2011. Fractalkine and CX 3 CR1 regulate hippocampal neurogenesis in adult and aged rats. Neurobiol. Aging 32, 2030–2044.

Balak, N., Elmaci, I., 2007. Costs of disorders of the brain in Europe. Eur. J. Neurol. 14, e9.

Belmaker, R.H., Agam, G., 2008. Major depressive disorder. N. Engl. J. Med. 358, 55–68.

Belsky, J., Pluess, M., 2009. Beyond diathesis stress: differential susceptibility to environmental influences. Psychol. Bull. 135, 885–908.

Belsky, J., Jonassaint, C., Pluess, M., Stanton, M., Brummett, B., Williams, R., 2009. Vulnerability genes or plasticity genes? Mol. Psychiatry 14, 746–754.

Bhavsar, P.K., Sukkar, M.B., Khorasani, N., Lee, K.Y., Chung, K.F., 2008. Glucocorticoid suppression of CX3CL1 (fractalkine) by reduced gene promoter recruitment of NF-kappaB. FASEB J. 22, 1807–1816.

Biber, K., Neumann, H., Inoue, K., Boddeke, H.W., 2007. Neuronal 'On' and 'Off' signals control microglia. Trends Neurosci. 30, 596–602.

Bilimoria, P.M., Stevens, B., 2015. Microglia function during brain development: new insights from animal models. Brain Res. 1617, 7–17.

Branchi, I., 2011. The double edged sword of neural plasticity: increasing serotonin levels leads to both greater vulnerability to depression and improved capacity to recover. Psychoneuroendocrinology 36, 339–351.

Branchi, I., Santarelli, S., Capoccia, S., Poggini, S., D'Andrea, I., Cirulli, F., Alleva, E., 2013a. Antidepressant treatment outcome depends on the quality of the living environment: a pre-clinical investigation in mice. PLoS One 8, e62226.

Branchi, I., Santarelli, S., D'Andrea, I., Alleva, E., 2013b. Not all stressors are equal: early social enrichment favors resilience to social but not physical stress in male mice. Horm. Behav. 63, 503–509.

Branchi, I., Alboni, S., Maggi, L., 2014. The role of microglia in mediating the effect of the environment in brain plasticity and behavior. Front. Cell. Neurosci. 8, 390.

Caspi, A., Sugden, K., Moffitt, T.E., Taylor, A., Craig, I.W., Harrington, H., McClay, J., Mill, J., Martin, J., Braithwaite, A., Poulton, R., 2003. Influence of life stress on depression: moderation by a polymorphism in the 5-HTT gene. Science 301, 386–389.

Chiarotti, F., Alleva, E., Bignami, G., 1987. Problems of test choice and data analysis in behavioral teratology: the case of prenatal benzodiazepines. Neurotoxicol. Teratol. 9, 179–186.

Christian, K.M., Miracle, A.D., Wellman, C.L., Nakazawa, K., 2011. Chronic stress-induced hippocampal dendritic retraction requires CA3 NMDA receptors. Neuroscience 174, 26–36.

Clark, A.K., Gruber-Schoffnegger, D., Drdla-Schutting, R., Gerhold, K.J., Malcangio, M., Sandkuhler, J., 2015. Selective activation of microglia facilitates synaptic strength. J. Neurosci. 35, 4552–4570.

Cohen, S., Janicki-Deverts, D., Miller, G.E., 2007. Psychological stress and disease. JAMA 298, 1685–1687.

Cook, S.C., Wellman, C.L., 2004. Chronic stress alters dendritic morphology in rat medial prefrontal cortex. J. Neurobiol. 60, 236–248.

Dalmau, I., Finsen, B., Zimmer, J., Gonzalez, B., Castellano, B., 1998. Development of microglia in the postnatal rat hippocampus. Hippocampus 8, 458–474.

Davidson, R.J., McEwen, B.S., 2012. Social influences on neuroplasticity: stress and interventions to promote well-being. Nat. Neurosci. 15, 689–695.

Donohue, H.S., Gabbott, P.L., Davies, H.A., Rodriguez, J.J., Cordero, M.I., Sandi, C., Medvedev, N.I., Popov, V.I., Colyer, F.M., Peddie, C.J., Stewart, M.G., 2006. Chronic restraint stress induces changes in synapse morphology in stratum lacunosum-moleculare CA1 rat hippocampus: a stereological and three-dimensional ultrastructural study. Neuroscience 140, 597–606.

Duman, R.S., Aghajanian, G.K., 2012. Synaptic dysfunction in depression: potential therapeutic targets. Science 338, 68–72.

Franklin, T.B., Saab, B.J., Mansuy, I.M., 2012. Neural mechanisms of stress resilience and vulnerability. Neuron 75, 747–761.

Gomez Perdiguero, E., Klapproth, K., Schulz, C., Busch, K., Azzoni, E., Crozet, L., Garner, H., Trouillet, C., de Bruijn, M.F., Geissmann, F., Rodewald, H.R., 2015. Tissue-resident macrophages originate from yolk-sac-derived erythro-myeloid progenitors. Nature 518, 547–551.

Goshen, I., Avital, A., Kreisel, T., Licht, T., Segal, M., Yirmiya, R., 2009. Environmental enrichment restores memory functioning in mice with impaired IL-1 signaling via reinstatement of long-term potentiation and spine size enlargement. J. Neurosci. 29, 3395–3403.

Hinwood, M., Morandini, J., Day, T.A., Walker, F.R., 2012. Evidence that microglia mediate the neurobiological effects of chronic psychological stress on the medial prefrontal cortex. Cereb. Cortex 22, 1442–1454.

Hinwood, M., Tynan, R.J., Charnley, J.L., Beynon, S.B., Day, T.A., Walker, F.R., 2013. Chronic stress induced remodeling of the prefrontal cortex: structural re-organization of microglia and the inhibitory effect of minocycline. Cereb. Cortex 23, 1784–1797.

Hodes, G.E., Brookshire, B.R., Hill-Smith, T.E., Teegarden, S.L., Berton, O., Lucki, I., 2012. Strain differences in the effects of chronic corticosterone exposure in the hippocampus. Neuroscience 222, 269–280.

Joels, M., Krugers, H.J., 2007. LTP after stress: up or down? Neural Plast. 2007, 93202.

Jung, S., Aliberti, J., Graemmel, P., Sunshine, M.J., Kreutzberg, G.W., Sher, A., Littman, D.R., 2000. Analysis of fractalkine receptor CX(3)CR1 function by targeted deletion and green fluorescent protein reporter gene insertion. Mol. Cell. Biol. 20, 4106–4114.

Kallarackal, A.J., Kvarta, M.D., Cammarata, E., Jaberi, L., Cai, X., Bailey, A.M., Thompson, S.M., 2013. Chronic stress induces a selective decrease in AMPA receptor-mediated synaptic excitation at hippocampal temporoammonic-CA1 synapses. J. Neurosci. 33, 15669–15674.

Karst, H., Joels, M., 2007. Brief RU 38486 treatment normalizes the effects of chronic stress on calcium currents in rat hippocampal CA1 neurons. Neuropsychopharmacology 32, 1830–1839.

Keck, T., Mrsic-Flogel, T.D., Vaz Afonso, M., Eysel, U.T., Bonhoeffer, T., Hubener, M., 2008. Massive restructuring of neuronal circuits during functional reorganization of adult visual cortex. Nat. Neurosci. 11, 1162–1167.

Kettenmann, H., Kirchhoff, F., Verkhratsky, A., 2013. Microglia: new roles for the synaptic stripper. Neuron 77, 10–18.

Kierdorf, K., Prinz, M., 2013. Factors regulating microglia activation. Front. Cell. Neurosci. 7, 44.

Kim, J.J., Diamond, D.M., 2002. The stressed hippocampus, synaptic plasticity and lost memories. Nat. Rev. Neurosci. 3, 453–462.

Kole, M.H., Czeh, B., Fuchs, E., 2004. Homeostatic maintenance in excitability of tree shrew hippocampal CA3 pyramidal neurons after chronic stress. Hippocampus 14, 742–751.

Koo, J.W., Duman, R.S., 2008. IL-1beta is an essential mediator of the antineurogenic and anhedonic effects of stress. Proc. Natl. Acad. Sci. U.S.A. 105, 751–756.

Kreisel, T., Frank, M.G., Licht, T., Reshef, R., Ben-Menachem-Zidon, O., Baratta, M.V., Maier, S.F., Yirmiya, R., 2014. Dynamic microglial alterations underlie stress-induced depressive-like behavior and suppressed neurogenesis. Mol. Psychiatry 19, 699–709.

Ligorio, M., Descarries, L., Warren, R.A., 2009. Cholinergic innervation and thalamic input in rat nucleus accumbens. J. Chem. Neuroanat. 37, 33–45.

Liston, C., Cichon, J.M., Jeanneteau, F., Jia, Z., Chao, M.V., Gan, W.B., 2013. Circadian glucocorticoid oscillations promote learning-dependent synapse formation and maintenance. Nat. Neurosci. 16, 698–705.

Luine, V., Villegas, M., Martinez, C., McEwen, B.S., 1994. Repeated stress causes reversible impairments of spatial memory performance. Brain Res. 639, 167–170.

Magarinos, A.M., McEwen, B.S., 1995. Stress-induced atrophy of apical dendrites of hippocampal CA3c neurons: involvement of glucocorticoid secretion and excitatory amino acid receptors. Neuroscience 69, 89–98.

Maggi, L., Scianni, M., Branchi, I., D'Andrea, I., Lauro, C., Limatola, C., 2011. CX(3)CR1 deficiency alters hippocampal-dependent plasticity phenomena blunting the effects of enriched environment. Front. Cell. Neurosci. 5, 22.

Majewska, A., Sur, M., 2003. Motility of dendritic spines in visual cortex in vivo: changes during the critical period and effects of visual deprivation. Proc. Natl. Acad. Sci. U.S.A. 100, 16024–16029.

Mayhew, J., Beart, P.M., Walker, F.R., 2015. Astrocyte and microglial control of glutamatergic signaling: a primer on understanding the disruptive role of chronic stress. J. Neuroendocrinol.

McEwen, B.S., 2007. Physiology and neurobiology of stress and adaptation: central role of the brain. Physiol. Rev. 87, 873–904.

Muller, N., 2014. Immunology of major depression. NeuroImmunoModulation 21, 123–130.

Musazzi, L., Racagni, G., Popoli, M., 2011. Stress, glucocorticoids and glutamate release: effects of antidepressant drugs. Neurochem. Int. 59, 138–149.

Nasca, C., Bigio, B., Zelli, D., Nicoletti, F., McEwen, B.S., 2014. Mind the gap: glucocorticoids modulate hippocampal glutamate tone underlying individual differences in stress susceptibility. Mol. Psychiatry.

O'Leary, O.F., Dinan, T.G., Cryan, J.F., 2015. Faster, better, stronger: towards new antidepressant therapeutic strategies. Eur. J. Pharmacol. 753, 32–50.

Paolicelli, R.C., Bolasco, G., Pagani, F., Maggi, L., Scianni, M., Panzanelli, P., Giustetto, M., Ferreira, T.A., Guiducci, E., Dumas, L., Ragozzino, D., Gross, C.T., 2011. Synaptic pruning by microglia is necessary for normal brain development. Science 333, 1456–1458.

Paolicelli, R.C., Bisht, K., Tremblay, M.E., 2014. Fractalkine regulation of microglial physiology and consequences on the brain and behaviour. Front. Cell. Neurosci. 8, 129.

Parkhurst, C.N., Yang, G., Ninan, I., Savas, J.N., Yates 3rd, J.R., Lafaille, J.J., Hempstead, B.L., Littman, D.R., Gan, W.B., 2013. Microglia promote learning-dependent synapse formation through brain-derived neurotrophic factor. Cell 155, 1596–1609.

Pawlak, R., Rao, B.S., Melchor, J.P., Chattarji, S., McEwen, B., Strickland, S., 2005. Tissue plasminogen activator and plasminogen mediate stress-induced decline of neuronal and cognitive functions in the mouse hippocampus. Proc. Natl. Acad. Sci. U.S.A. 102, 18201–18206.

Paxinos, G., Franklin, K.B., 2013. The Mouse Brain in Stereotaxic Coordinates. Academic Press, New York.

Penzes, P., Cahill, M.E., Jones, K.A., VanLeeuwen, J.E., Woolfrey, K.M., 2011. Dendritic spine pathology in neuropsychiatric disorders. Nat. Neurosci. 14, 285–293.

Peters, A., Palay, S.L., Webster, H., 1991. The Fine Structure of the Nervous System: the Neurons and Supporting Cells. W. B. Saunders, Philadelphia.

Petersen, C.C., Malenka, R.C., Nicoll, R.A., Hopfield, J.J., 1998. All-or-none potentiation at CA3–CA1 synapses. Proc. Natl. Acad. Sci. U.S.A. 95, 4732–4737.

Pfau, M.L., Russo, S.J., 2015. Peripheral and central mechanisms of stress resilience. Neurobiol. Stress 1, 66–79.

Radley, J.J., Sisti, H.M., Hao, J., Rocher, A.B., McCall, T., Hof, P.R., McEwen, B.S., Morrison, J.H., 2004. Chronic behavioral stress induces apical dendritic reorganization in pyramidal neurons of the medial prefrontal cortex. Neuroscience 125, 1–6.

Radley, J.J., Rocher, A.B., Miller, M., Janssen, W.G., Liston, C., Hof, P.R., McEwen, B.S., Morrison, J.H., 2006. Repeated stress induces dendritic spine loss in the rat medial prefrontal cortex. Cereb. Cortex 16, 313–320.

Reaux-Le Goazigo, A., Van Steenwinckel, J., Rostene, W., Melik Parsadaniantz, S., 2013. Current status of chemokines in the adult CNS. Prog. Neurobiol. 104, 67–92.

Reshef, R., Kreisel, T., Beroukhim Kay, D., Yirmiya, R., 2014. Microglia and their CX3CR1 signaling are involved in hippocampal – but not olfactory bulb-related memory and neurogenesis. Brain Behav. Immun. 41, 239–250.

Rogers, J.T., Morganti, J.M., Bachstetter, A.D., Hudson, C.E., Peters, M.M., Grimmig, B.A., Weeber, E.J., Bickford, P.C., Gemma, C., 2011. CX3CR1 deficiency leads to impairment of hippocampal cognitive function and synaptic plasticity. J. Neurosci. 31, 16241–16250.

Rubenstein, J.L., Merzenich, M.M., 2003. Model of autism: increased ratio of excitation/inhibition in key neural systems. Genes Brain Behav. 2, 255–267.

Sandi, C., 2011. Glucocorticoids act on glutamatergic pathways to affect memory processes. Trends Neurosci. 34, 165–176.

Schafer, D.P., Lehrman, E.K., Kautzman, A.G., Koyama, R., Mardinly, A.R., Yamasaki, R., Ransohoff, R.M., Greenberg, M.E., Barres, B.A., Stevens, B., 2012. Microglia sculpt postnatal neural circuits in an activity and complement-dependent manner. Neuron 74, 691–705.

Schweizer, M.C., Henniger, M.S., Sillaber, I., 2009. Chronic mild stress (CMS) in mice: of anhedonia, 'anomalous anxiolysis' and activity. PLoS One 4, e4326.

Shabel, S.J., Proulx, C.D., Piriz, J., Malinow, R., 2014. Mood regulation. GABA/glutamate co-release controls habenula output and is modified by antidepressant treatment. Science 345, 1494–1498.

Sheridan, G.K., Murphy, K.J., 2013. Neuron-glia crosstalk in health and disease: fractalkine and CX3CR1 take centre stage. Open Biol. 3, 130181.

Sierra, A., Beccari, S., Diaz-Aparicio, I., Encinas, J.M., Comeau, S., Tremblay, M.E., 2014a. Surveillance, phagocytosis, and inflammation: how never-resting microglia influence adult hippocampal neurogenesis. Neural Plast. http://dx.doi.org/10.1155/2014/610343. Article ID 610343 (15 pages).

Sierra, A., Tremblay, M.E., Wake, H., 2014b. Never-resting microglia: physiological roles in the healthy brain and pathological implications. Front. Cell. Neurosci. 8, 240.

Tremblay, M.E., Riad, M., Bouvier, D., Murai, K.K., Pasquale, E.B., Descarries, L., Doucet, G., 2007. Localization of EphA4 in axon terminals and dendritic spines of adult rat hippocampus. J. Comp. Neurol. 501, 691–702.

Tremblay, M.E., Riad, M., Chierzi, S., Murai, K.K., Pasquale, E.B., Doucet, G., 2009. Developmental course of EphA4 cellular and subcellular localization in the postnatal rat hippocampus. J. Comp. Neurol. 512, 798–813.

Tremblay, M.E., Lowery, R.L., Majewska, A.K., 2010a. Microglial interactions with synapses are modulated by visual experience. PLoS Biol. 8, e1000527.

Tremblay, M.E., Riad, M., Majewska, A., 2010b. Preparation of mouse brain tissue for immunoelectron microscopy. J. Vis. Exp. – JoVE.

Tremblay, M.E., Stevens, B., Sierra, A., Wake, H., Bessis, A., Nimmerjahn, A., 2011. The role of microglia in the healthy brain. J. Neurosci. 31, 16064–16069.

Tremblay, M.E., Zettel, M.L., Ison, J.R., Allen, P.D., Majewska, A.K., 2012. Effects of aging and sensory loss on glial cells in mouse visual and auditory cortices. Glia 60, 541–558.

Tynan, R.J., Naicker, S., Hinwood, M., Nalivaiko, E., Buller, K.M., Pow, D.V., Day, T.A., Walker, F.R., 2010. Chronic stress alters the density and morphology of microglia in a subset of stress-responsive brain regions. Brain Behav. Immun. 24, 1058–1068.

Venero, C., Borrell, J., 1999. Rapid glucocorticoid effects on excitatory amino acid levels in the hippocampus: a microdialysis study in freely moving rats. Eur. J. Neurosci. 11, 2465–2473.

Walker, F.R., Nilsson, M., Jones, K., 2013. Acute and chronic stress-induced disturbances of microglial plasticity, phenotype and function. Curr. Drug Targets 14, 1262–1276.

Wilcox, R.R., 1987. New Statistical Procedures for the Social Sciences. Modern Solutions to Basic Problems. Lawrence Erlbaum, Hillsdale, NJ, USA.

Wohleb, E.S., Powell, N.D., Godbout, J.P., Sheridan, J.F., 2013. Stress-induced recruitment of bone marrow-derived monocytes to the brain promotes anxiety-like behavior. J. Neurosci. 33, 13820–13833.

Yoon, T., Okada, J., Jung, M.W., Kim, J.J., 2008. Prefrontal cortex and hippocampus subserve different components of working memory in rats. Learn. Mem. 15, 97–105.

Yuen, E.Y., Wei, J., Liu, W., Zhong, P., Li, X., Yan, Z., 2012. Repeated stress causes cognitive impairment by suppressing glutamate receptor expression and function in prefrontal cortex. Neuron 73, 962–977.

Zhan, Y., Paolicelli, R.C., Sforazzini, F., Weinhard, L., Bolasco, G., Pagani, F., Vyssotski, A.L., Bifone, A., Gozzi, A., Ragozzino, D., Gross, C.T., 2014. Deficient neuron–microglia signaling results in impaired functional brain connectivity and social behavior. Nat. Neurosci.

Zucker, R.S., 1989. Short-term synaptic plasticity. Annu. Rev. Neurosci. 12, 13–31.